Effects of Variable Viscosity on the Peristaltic Motion in a Third-Order Fluid

Sohail Nadeem[a], Noreen Sher Akbar[a], and Tasawar Hayat[a,b]

[a] Department of Mathematics, Quaid-i-Azam University 45320, Islamabad 44000, Pakistan
[b] Department of Mathematics, College of Sciences, King Saud University, P. O. Box 2455, Riyadh 11451, Saudi Arabia

Reprint requests to S. N.; Fax: +92 512275341; E-mail: snqau@hotmail.com

Z. Naturforsch. **65a,** 901 – 910 (2010); received July 13, 2009 / revised December 10, 2009

This article deals with the variable viscosity effects on the channel flow of a third-order fluid. The walls of the asymmetric channel are of different temperatures. Continuity, momentum, and energy equations are utilized in the mathematical analysis. Three types of solutions, namely, the perturbation, homotopy analysis, and numerical are derived. These solutions are compared. The perturbation, homtopy analysis, and numerical solutions are identical up to three digits. The expressions for pressure rise and frictional forces have been calculated using numerical integration. The expressions for pressure rise, frictional forces, velocity profile, temperature profile, pressure gradient, and streamlines have been discussed graphically at the end of the article.

Key words: Variable Viscosity; Shooting Method; Comparison.

1. Introduction

The peristaltic flow has paramount importance in physiology and engineering science. Occurrence of such flows are quite prevalent in nature. Particularly, these flows are encountered in the urinary tract, chyme movement in the gastrointestinal tract, swallowing of food through esophagus, and many others. The pioneering work on this topic has been initiated by Latham [1] and most investigators over the last few decades have been stimulated to discuss the peristaltic flows of viscous and non-Newtonian fluids in symmetric/asymmetric channels. Few recent studies [1 – 16] and several references therein can shed light in this direction.

The works cited thus far as regards to the peristaltic flows suggests that such problems in the regime of variable viscosity of fluid is scarcely studied. Hence, due to such limitations it is appropriate to look at more realistic situations in peristaltic flows. Therefore, the present paper is organized as follows. The next section presents the mathematical formulation. Section 3 consists of perturbation, homotopy analysis, and numerical solutions of the arising problem. The shapes of different wave forms are also prescribed in the same section. The interpretation relevant to graphs is given in Section 4. Section 5 contains the summery of the conducted work.

2. Mathematical Formulation

Let us investigate the peristaltic flow of a third-order fluid in an asymmetric channel. Asymmetry in the flow is caused by the propagation of peristaltic waves of different amplitudes and phases on the channel walls. The heat transfer in the channel is taken into account by giving temperature to the upper and lower walls as T_0 and T_1, respectively. The shapes of the channel walls are represented by the following expressions:

$$\begin{aligned} Y = H_1 &= d_1 + a_1 \cos\left[\frac{2\pi}{\lambda}(X - ct)\right], \\ Y = H_2 &= -d_2 - b_1 \cos\left[\frac{2\pi}{\lambda}(X - ct) + \phi\right]. \end{aligned} \tag{1}$$

In above equations a_1 and b_1 are the waves amplitudes, λ is the wave length, $d_1 + d_2$ the channel width, c the wave speed, t the time, and X the direction of wave propagation (see Fig. 1). The phase difference ϕ varies in the range $0 \leq \phi \leq \pi$. When $\phi = 0$ then a symmetric channel with waves out of phase can be described and for $\phi = \pi$, the waves are in phase. Moreover, a_1, b_1, d_1, d_2, and ϕ meet the relation

$$a_1^2 + b_1^2 + 2a_1 b_1 \cos\phi \leq (d_1 + d_2)^2.$$

For two-dimensional flow, the continuity, momentum

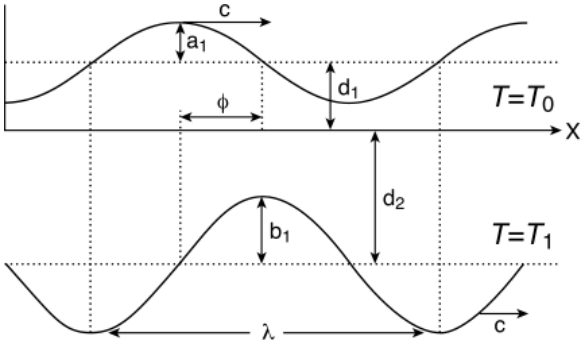

Fig. 1. Geometry of the problem.

and energy equations yield

$$\frac{\partial U}{\partial X}+\frac{\partial V}{\partial Y}=0, \tag{2}$$

$$\rho\left(\frac{\partial U}{\partial t}+U\frac{\partial U}{\partial X}+V\frac{\partial U}{\partial Y}\right)= -\frac{\partial p}{\partial X}+\frac{\partial}{\partial X}(S_{XX})+\frac{\partial}{\partial Y}(S_{XY}), \tag{3}$$

$$\rho\left(\frac{\partial V}{\partial t}+U\frac{\partial V}{\partial X}+V\frac{\partial V}{\partial Y}\right)= -\frac{\partial p}{\partial Y}+\frac{\partial}{\partial X}(S_{YX})+\frac{\partial}{\partial Y}(S_{YY}), \tag{4}$$

$$C'\left(\frac{\partial T}{\partial t}+U\frac{\partial T}{\partial X}+V\frac{\partial T}{\partial Y}\right)=\frac{K'}{\rho}\nabla^2 T+\upsilon\Phi, \tag{5}$$

$$\nabla^2=\frac{\partial^2}{\partial X^2}+\frac{\partial^2}{\partial Y^2},$$

in which U, V denote the velocities in X and Y-directions in the fixed frame, ρ is the constant density, p the pressure, K' the thermal conductivity, C' the specific heat, T the temperature, and $\upsilon\Phi$ the dissipation factor.

The expression of extra stress tensor $\bar{\mathbf{S}}$ is

$$\bar{\mathbf{S}}=(\mu+\beta_3\mathrm{tr}\bar{\mathbf{A}}_1^2)\bar{\mathbf{A}}_1+\alpha_1\bar{\mathbf{A}}_2+\alpha_2\bar{\mathbf{A}}_1^2 +\beta_1\bar{\mathbf{A}}_3+\beta_2(\bar{\mathbf{A}}_1\bar{\mathbf{A}}_2+\bar{\mathbf{A}}_2\bar{\mathbf{A}}_1), \tag{6}$$

where μ, α_i $(i=1,2)$ and β_i $(i=1,2,3)$ are the material constants. The Rivlin-Ericksen tensors can be computed by invoking the following relations:

$$\bar{\mathbf{A}}_1=\bar{\mathbf{L}}+\bar{\mathbf{L}}^{\mathrm{t}},$$

$$\bar{\mathbf{A}}_{n+1}=\frac{\mathrm{d}\bar{\mathbf{A}}_n}{\mathrm{d}\bar{t}}+\bar{\mathbf{A}}_n\bar{\mathbf{L}}+\bar{\mathbf{L}}^{\mathrm{t}}\bar{\mathbf{A}}_n,\quad n=1,2,$$

where $\bar{\mathbf{L}}=\mathrm{grad}\,\bar{\mathbf{V}}$ and t indicates the matrix transpose.

Note that $\mu(y)$ is the variable viscosity, λ_1 the ratio of relaxation to retardation times, $\dot{\gamma}$ the shear rate, λ_2 the retardation time, and dots denote the differentiation with respect to time.

The transformations between the laboratory and the wave frames are

$$x=X-ct,\quad y=Y,\quad u=U-c,\quad v=V,\quad p(x)=p(X,t), \tag{7}$$

where (x,y), (u,v), and p are the notations in the wave frame.

If Ψ is the stream function defined by

$$u=\frac{\partial\Psi}{\partial y},\quad v=-\delta\frac{\partial\Psi}{\partial x}$$

and using

$$\begin{aligned}
&\bar{x}=\frac{2\pi x}{\lambda},\quad \bar{y}=\frac{y}{d_1},\quad \bar{u}=\frac{u}{c},\quad \bar{v}=\frac{v}{c\delta},\\
&\delta=\frac{d_1}{\lambda},\quad d=\frac{d_2}{d_1},\quad \bar{p}=\frac{d_1^2 p}{\mu_0 c\lambda},\quad h_1=\frac{H_1}{d_1},\\
&\bar{t}=\frac{ct}{\lambda},\quad h_2=\frac{H_2}{d_2},\quad a=\frac{a_1}{d_1},\quad b=\frac{b_1}{d_1},\\
&Re=\frac{cd_1}{\nu},\quad \bar{\Psi}=\frac{\Psi}{cd_1},\quad \theta=\frac{T-T_0}{T_1-T_0},\\
&Ec=\frac{c^2}{C'(T_1-T_0)},\quad Pr=\frac{\rho\nu C'}{K'},\quad \bar{S}=\frac{Sd_1}{\mu_0 c},\\
&\lambda_1=\frac{\alpha_1 c}{\mu_0 d_1},\quad \mu(y)=\frac{\mu(Y)}{\mu_0},\quad \gamma_1=\frac{\beta_1 c^2}{\mu_0 d_1^2},\\
&\gamma_2=\frac{\beta_2 c^2}{\mu_0 d_1^2},\quad \gamma_3=\frac{\beta_3 c^2}{\mu_0 d_1^2},\quad \lambda_2=\frac{\alpha_2 c}{\mu_0 d_1},\\
&\Gamma=\gamma_2+\gamma_3,
\end{aligned} \tag{8}$$

then with (7) we have

$$\frac{\partial^2}{\partial y^2}\left[\mu(y)\frac{\partial^2\Psi}{\partial y^2}+2\Gamma\left(\frac{\partial^2\Psi}{\partial y^2}\right)^3\right]=0, \tag{9}$$

$$\frac{\mathrm{d}p}{\mathrm{d}x}=\frac{\partial}{\partial y}\left[\mu(y)\frac{\partial^2\Psi}{\partial y^2}+2\Gamma\left(\frac{\partial^2\Psi}{\partial y^2}\right)^3\right], \tag{10}$$

$$\frac{\partial^2\theta}{\partial y^2}+Br\left[\mu(y)+2\Gamma\left(\frac{\partial^2\Psi}{\partial y^2}\right)^2\right]\left(\frac{\partial^2\Psi}{\partial y^2}\right)^2=0. \tag{11}$$

The subjected boundary conditions are

$$\Psi=\frac{F}{2}\ \text{ at }\ y=h_1=1+a\cos x,$$

$$\Psi=-\frac{F}{2},\ \text{ at }\ y=h_2=-d-b\cos(x+\phi),$$

$$\begin{aligned}&\frac{\partial \Psi}{\partial y} = -1 \ \text{ at } \ y = h_1 \ \text{ and } \ y = h_2,\\ &\theta = 0 \ \text{ at } \ y = h_1,\\ &\theta = 1 \ \text{ at } \ y = h_2,\end{aligned} \tag{12}$$

where flux in the wave frame is denoted by F and a, b, ϕ, and d satisfy the following expression:

$$a^2 + b^2 + 2ab\cos\phi \le (1+d)^2,$$

where $p \neq p(y)$ and the long wavelength assumption is used in writing the above equations. In the fixed frame the flux at any axial station is written as

$$\begin{aligned}\bar{Q} &= \int_{h2}^{h1} (u+1)\mathrm{d}y = \int_{h2}^{h1} u\mathrm{d}y + \int_{h2}^{h1} \mathrm{d}y\\ &= F + h_1 - h_2.\end{aligned} \tag{13}$$

The average volume flow rate over one period $\left(T = \frac{\lambda}{c}\right)$ of the peristaltic wave is given by the following expression:

$$\begin{aligned}Q &= \frac{1}{T}\int_0^T \bar{Q}\mathrm{d}t = \frac{1}{T}\int_0^T (q + h_1 - h_2)\mathrm{d}t\\ &= F + 1 + d.\end{aligned} \tag{14}$$

3. Solution of the Problem

This section aims to derive the solutions by perturbation, homotopy analysis, and shooting methods.

3.1. Perturbation Solution

The value of variable viscosity is chosen as follows [3]:

$$\mu(y) = \mathrm{e}^{-\alpha y} \approx 1 - \alpha y, \tag{15}$$

where α is constant.

For small Deborah number, the solutions of stream function, temperature, and axial pressure gradient are

$$\begin{aligned}\Psi &= L_{109}y^4 + L_{110}y^3 + L_{111}y^2 + L_3 y + L_4\\ &\quad + \Gamma(L_{12}y^9 + L_{13}y^8 + L_{14}y^7 + L_{15}y^6 + L_{16}y^5),\end{aligned} \tag{16}$$

$$\begin{aligned}\theta &= L_{29}y^7 + L_{30}y^6 + L_{31}y^5 + L_{32}y^4 + L_{33}y^3\\ &\quad + L_{34}y^2 + L_{37}y + L_{38} + \Gamma(L_{89}y^{17} + L_{90}y^{16}\\ &\quad + L_{91}y^{15} + L_{92}y^{14} + L_{93}y^{13} + L_{94}y^{12}\\ &\quad + L_{95}y^{11} + L_{96}y^{10} + L_{97}y^9 + L_{98}y^8),\end{aligned} \tag{17}$$

$$\begin{aligned}\frac{\mathrm{d}p}{\mathrm{d}x} &= -36(F + h_1 - h_2)(2 + (h_1 + h_2)\alpha)\left[(h_1 - h_2)^3\right.\\ &\quad \left.\cdot(6 + 6(h_1 + h_2)\alpha + (h_1^2 + 4h_1h_2 + h_2^2)\alpha^2)\right]^{-1}\\ &\quad + \Gamma(L_{54}),\end{aligned} \tag{18}$$

where the involved L_i ($i = 1 - 111$) are presented in the Appendix.

The dimensionless pressure rise Δp satisfies the following equation:

$$\Delta p = \int_0^1 \left(\frac{\mathrm{d}p}{\mathrm{d}x}\right)\mathrm{d}x. \tag{19}$$

3.2. Solution by Homotopy Analysis Method (HAM)

For HAM solution, the initial guess Ψ_0 and auxiliary linear operators $L_{\Psi y}$ are chosen in the form

$$\begin{aligned}\Psi_0 &= \frac{(F + h_1 - h_2)}{(h_2 - h_1)^3}(2y^3 - 3h_1y^2 - 3h_2y^2 + 6h_1h_2y)\\ &\quad - y + \frac{1}{(h_2 - h_1)^3}\left[\left(\frac{F}{2} + h_1\right)(h_2^3 - 3h_1h_2^2)\right.\\ &\quad \left.-\left(h_2 - \frac{F}{2}\right)(h_1^3 - 3h_1^2h_2)\right],\end{aligned} \tag{20}$$

$$\mathcal{L}_{\Psi y}(\Psi) = \Psi'''', \tag{21}$$

$$\mathcal{L}_{\Psi y}(\Psi_0) = 0. \tag{22}$$

The zeroth-order deformation problems are

$$(1-q)\mathcal{L}_{\Psi y}[\,\bar{\Psi}(y,q) - \Psi_0(y)] = q\hbar_\Psi N_{\Psi y}[\bar{\Psi}(y,q)], \tag{23}$$

$$\begin{aligned}&\bar{\Psi}(y,q) = \frac{F}{2} \ \text{ at } \ y = h_1 = 1 + a\sin x,\\ &\bar{\Psi}(y,q) = -\frac{F}{2} \ \text{ at } \ y = h_2 = -d - b\sin(x+\phi),\\ &\frac{\partial \bar{\Psi}(y,q)}{\partial y} = -1 \ \text{ at } \ y = h_1 \ \text{ and } \ y = h_2,\end{aligned} \tag{24}$$

where $\hbar_\Psi$ denotes the non-zero auxiliary parameter, $q \in [0,1]$ is an embedding parameter, and the nonlinear operator $N_{\Psi y}$ is

$$\begin{aligned}N_{\Psi y}[\bar{\Psi}(y,q)] &= (1-\alpha y)\frac{\partial^4 \Psi}{\partial y^4} + 6\Gamma\left(\frac{\partial^2 \Psi}{\partial y^2}\right)^2\frac{\partial^4 \Psi}{\partial y^4}\\ &\quad -2\alpha\frac{\partial^3 \Psi}{\partial y^3} + 12\Gamma\frac{\partial^2 \Psi}{\partial y^2}\left(\frac{\partial^3 \Psi}{\partial y^3}\right)^2.\end{aligned} \tag{25}$$

Obviously, when q varies from 0 to 1, then $\bar{\Psi}(y,q)$ varies from the initial guess Ψ_0 to the solution $\Psi(y)$.

y	Perturbation Sol.	Numerical Sol.	Error	HAM Sol.	Error
−1.0	−1.00000	−1.00000	0.00000	−1.00000	0.00000
−0.8	−1.11088	−1.10906	0.00160	−1.11080	0.00156
−0.6	−1.19564	−1.19244	0.00267	−1.19566	0.00269
−0.4	−1.25540	−1.25123	0.00332	−1.25542	0.00333
−0.2	−1.29092	−1.28619	0.00366	−1.29090	0.00364
0.0	−1.30268	−1.29778	0.00363	−1.30265	0.00286
0.2	−1.29082	−1.28614	0.00362	−1.29080	0.00361
0.4	−1.25519	−1.25114	0.00322	−1.25517	0.00321
0.6	−1.19535	−1.19234	0.00251	−1.19534	0.00250
0.8	−1.11061	−1.10904	0.00141	−1.11060	0.00140
1.0	−1.00000	−1.00000	0.00000	−1.00000	0.00000

Table 1. Comparison of solutions by various methods for $h=-1$, $a=0.5$, $b=0.4$, $d=1$, $\alpha=0.6$, $\phi=\frac{\pi}{2}$, $x=-\pi$, and $\Gamma=0.1$.

Expanding $\bar{\Psi}(y,q)$ in Taylor's series with respect to an embedding parameter q, we have

$$\bar{\Psi}(y,q)=\Psi_0(y)+\sum_{n=1}^{\infty}\Psi_m(y)q^m, \tag{26}$$

$$\Psi_m=\frac{1}{m!}\left.\frac{\partial^m\bar{\Psi}(y,q)}{\partial q^m}\right|_{q=0}. \tag{27}$$

The problems at mth-order are

$$\mathcal{L}_\Psi[\Psi_m(y)-\chi_m\Psi_{m-1}(y)]=\hbar_\Psi R_{\Psi y}(y), \tag{28}$$

$$\begin{aligned}R_{\Psi y}&=(1-\alpha y)\Psi_{m-1}''''\\&+6\Gamma\sum_{i=0}^{m-1}\Psi_{m-1}''''\Psi_{m-1-i}''\Psi_{m-i}''-2\alpha\sum_{i=0}^{m-1}\Psi_{m-1}'''\\&+12\sum_{i=0}^{m-1}\Psi_{m-1}''\Psi_{m-1-i}'''\Psi_{m-i}'''\end{aligned} \tag{29}$$

$$\chi_m=\begin{cases}0, & m\le 1,\\ 1, & m>1.\end{cases} \tag{30}$$

By Mathematica the solution can be computed as

$$\begin{aligned}\Psi_m(y)=&\lim_{M\to\infty}\left[\sum_{n=1}^{2M+1}\left(\sum_{m=n-1}^{2M}\sum_{k=0}^{2m+1-n}a_{m,n}^k y^{2n+3}\right)\right]\\&+\lim_{M\to\infty}\left[\sum_{m=0}^{M}a_{m,0}^0\right],\end{aligned} \tag{31}$$

where $a_{m,0}^0$ and $a_{m,n}^k$ are the constants.

3.3. Numerical Solution

Here the shooting method is used to solve (9) and (12) numerically. Moreover, the numerical solution is compared with the perturbation and the homotopy solutions. The values of the different solutions are presented in Table 1.

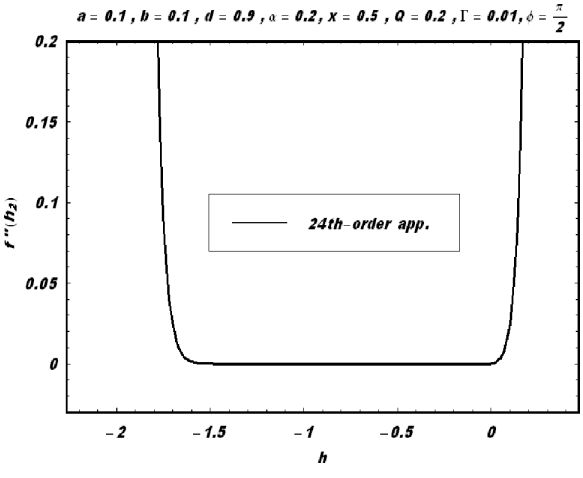

Fig. 2. h-curve for the velocity profile; parameters: $a=0.1$, $b=0.1$, $d=0.9$, $\alpha=0.2$, $x=0.5$, $Q=0.2$, $\Gamma=0.01$, $\phi=\pi/2$.

3.4. Expressions for Wave Shapes

The non-dimensional expressions for the three considered wave forms are given by

i) Sinusoidal wave

$$h(x)=1+\phi\cos 2\pi x.$$

ii) Triangular wave

$$h(x)=1+\phi\left[\frac{8}{\pi^3}\sum_{m=1}^{\infty}\frac{(-1)^{m+1}}{(2m-1)^2}\cos[2(2m-1)\pi x]\right].$$

iii) Trapezoidal wave

$$h(x)=1+\phi\left[\frac{32}{\pi^2}\sum_{m=1}^{\infty}\frac{\sin\left[\frac{\pi}{8}(2m-1)\right]}{(2m-1)^2}\cos[2(2m-1)\pi x]\right].$$

4. Graphical Results and Discussion

This section describes the graphical representation of the derived solutions. Figure 2 shows the convergence of the velocity profile. A comparative study has

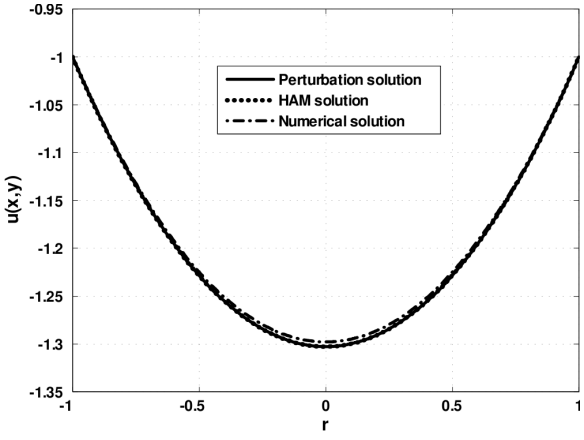

Fig. 3. Comparison of the velocity field for $h=-1$, $a=0.5$, $b=0.4$, $d=1$, $\alpha=0.6$, $\phi=\frac{\pi}{2}$, $x=-\pi$, $\Gamma=0.1$.

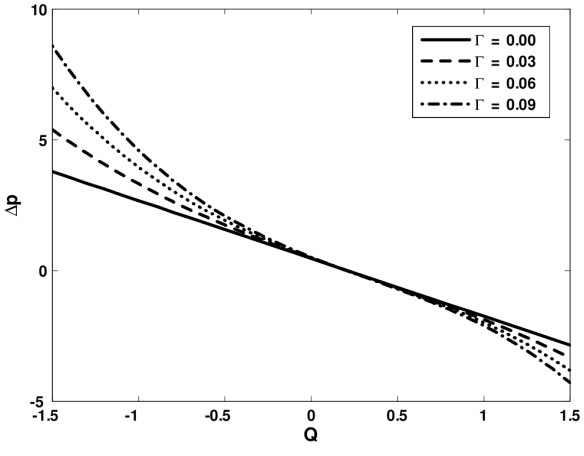

Fig. 4. Pressure rise versus flow rate for $a=0.2$, $b=0.5$, $d=0.9$, $\alpha=0.2$, $\phi=\frac{\pi}{2}$.

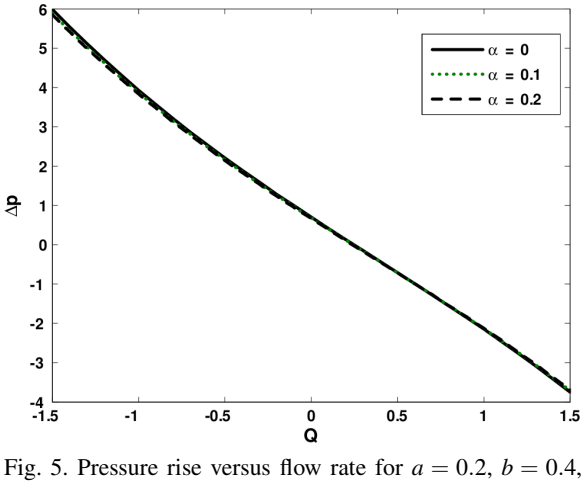

Fig. 5. Pressure rise versus flow rate for $a=0.2$, $b=0.4$, $d=0.8$, $\Gamma=0.01$, $\phi=0.8$.

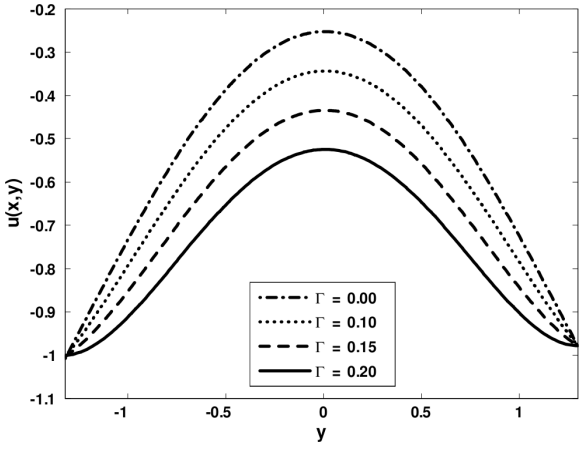

Fig. 6. Velocity field for $a=0.5$, $b=0.4$, $d=1$, $\alpha=0.01$, $\phi=\frac{\pi}{2}$, $x=-\pi$, $Q=1$.

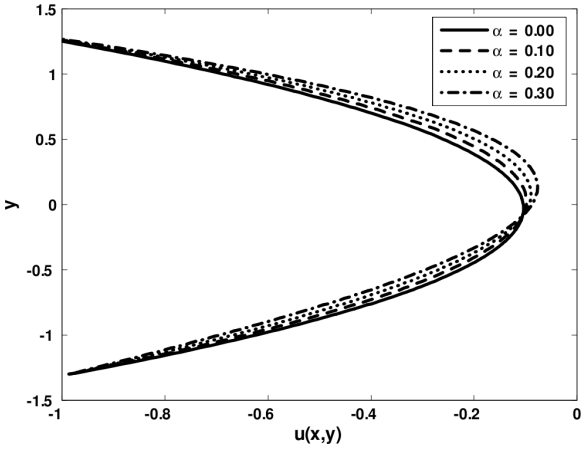

Fig. 7. Velocity field for $a=0.4$, $b=0.4$, $d=1$, $\Gamma=0.01$, $\phi=\frac{\pi}{2}$, $x=-\pi$, $Q=1$.

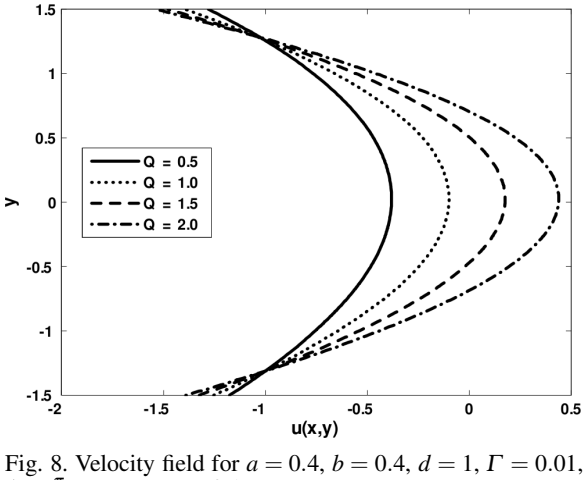

Fig. 8. Velocity field for $a=0.4$, $b=0.4$, $d=1$, $\Gamma=0.01$, $\phi=\frac{\pi}{2}$, $x=-\pi$, $\alpha=0.1$.

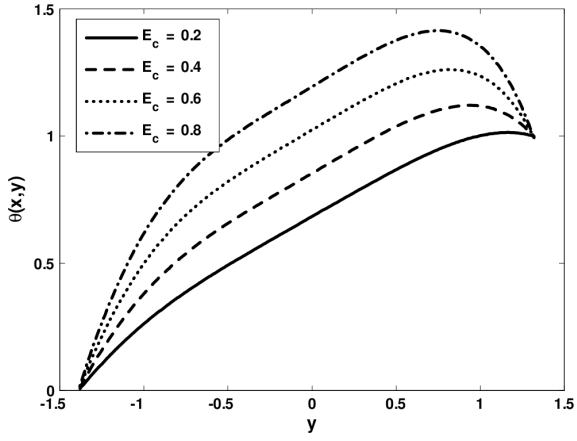

Fig. 9. Temperature profile for $a = 0.5$, $b = 0.5$, $d = 1$, $\Gamma = 0.02$, $\phi = \frac{\pi}{2}$, $x = -\pi$, $\alpha = 0.01$, $Q = 1$, $Pr = 0.5$.

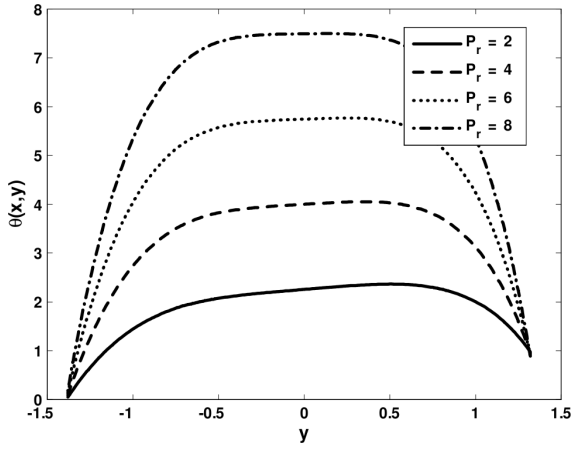

Fig. 10. Temperature profile for $a = 0.5$, $b = 0.5$, $d = 1$, $\Gamma = 0.02$, $\phi = \frac{\pi}{2}$, $x = -\pi$, $\alpha = 0.01$, $Q = 1$, $Ec = 0.5$.

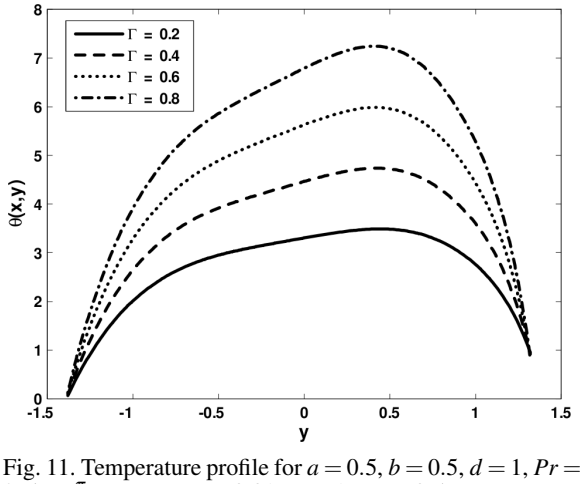

Fig. 11. Temperature profile for $a = 0.5$, $b = 0.5$, $d = 1$, $Pr = 2$, $\phi = \frac{\pi}{2}$, $x = -\pi$, $\alpha = 0.01$, $Q = 1$, $Ec = 0.5$.

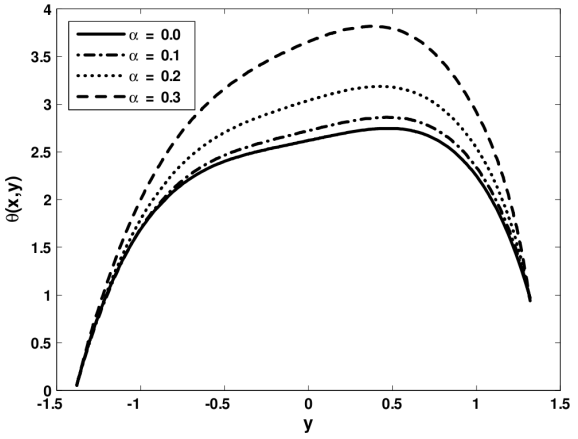

Fig. 12. Temperature profile for $\Gamma = 0.5$, $b = 0.5$, $d = 1$, $Pr = 2$, $\phi = \frac{\pi}{2}$, $x = -\pi$, $\alpha = 0.01$, $Q = 1$, $Ec = 0.5$.

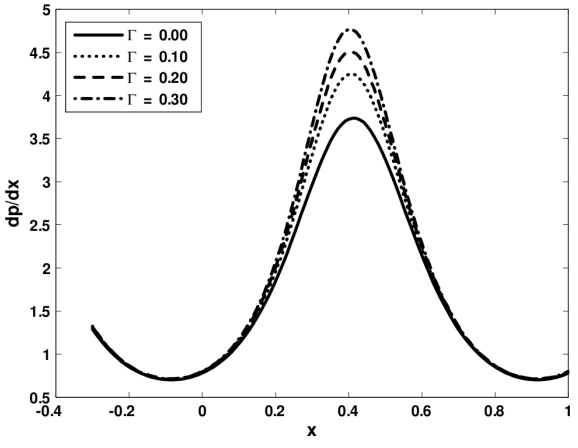

Fig. 13. Pressure gradient versus x for $\alpha = 0.2$, $b = 0.5$, $d = 1$, $\phi = \frac{\pi}{2}$, $\alpha = 0.01$, $Q = 1$.

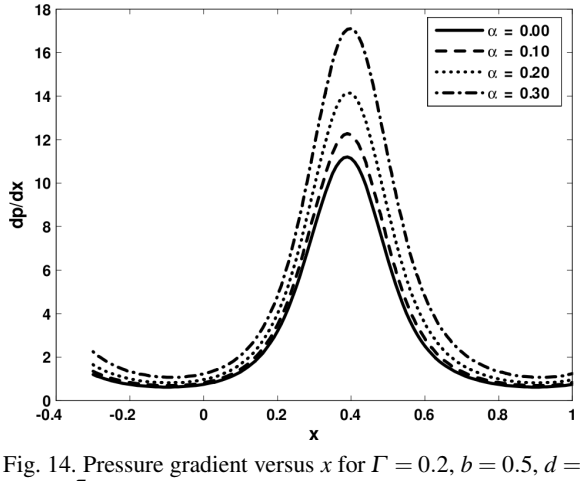

Fig. 14. Pressure gradient versus x for $\Gamma = 0.2$, $b = 0.5$, $d = 1$, $\phi = \frac{\pi}{2}$, $\alpha = 0.01$, $Q = 1$.

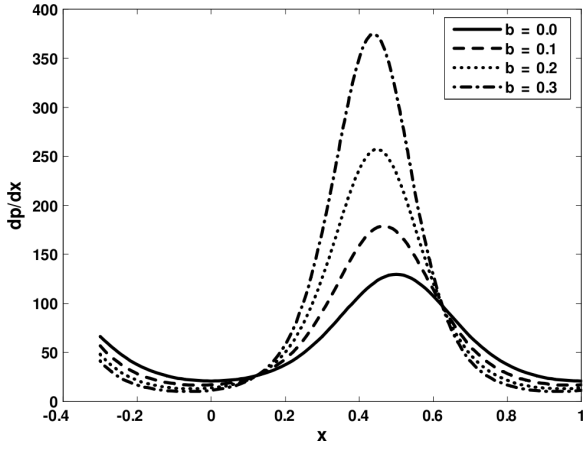

Fig. 15. Pressure gradient versus x for $\alpha = 0.2$, $\Gamma = 0.5$, $d = 1$, $\phi = \frac{\pi}{2}$, $\alpha = 0.01$, $Q = 1$.

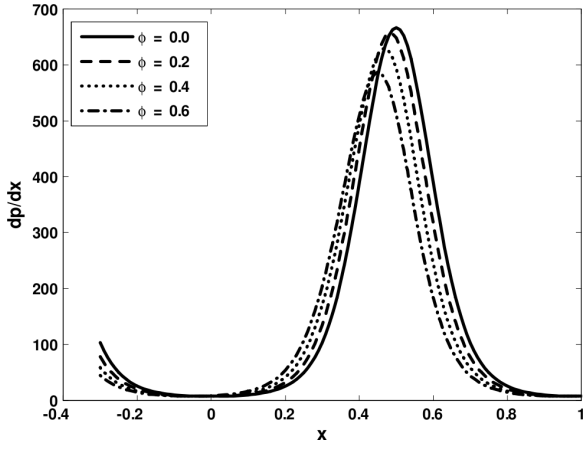

Fig. 16. Pressure gradient versus x for $\alpha = 0.2$, $\Gamma = 0.5$, $d = 1$, $b = 0.5$, $\alpha = 0.01$, $Q = 1$.

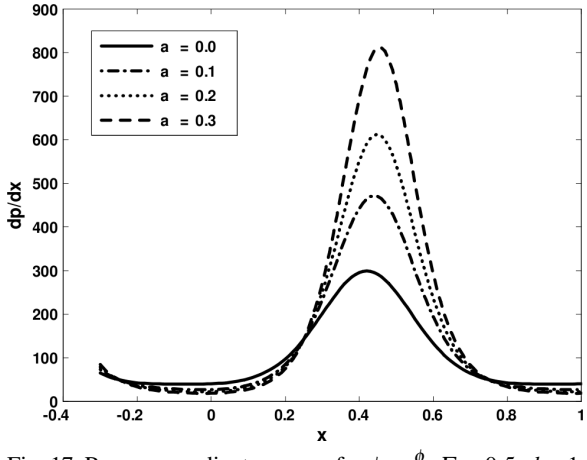

Fig. 17. Pressure gradient versus x for $\phi = \frac{\phi}{2}$, $\Gamma = 0.5$, $d = 1$, $b = 0.5$, $\alpha = 0.01$, $Q = 1$.

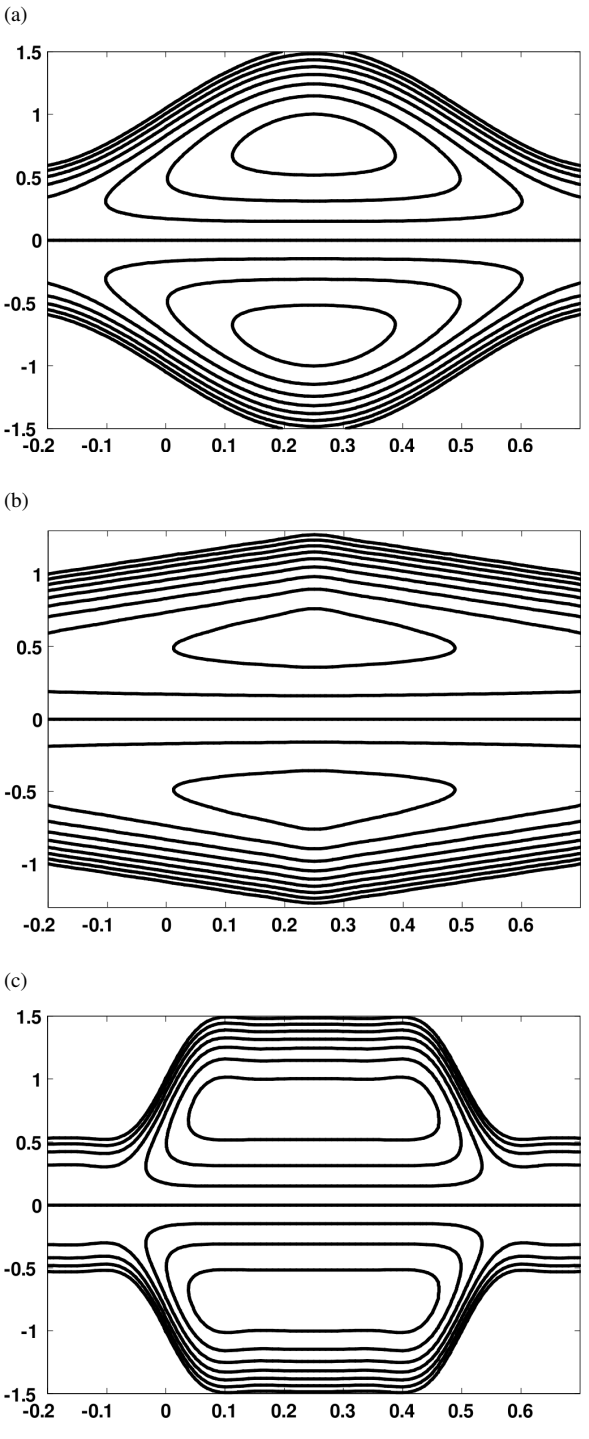

Fig. 18. Stream lines for (a) sinusoidal wave, (b) triangular wave, (c) trapezoidal wave; parameters: $a = 0.5$, $b = 0.5$, $d = 1.0$, $\Gamma = 0.02$, $\alpha = 0.2$, $Q = 1.8$, $\phi = 0.02$

been made for three solutions and is shown through Table 1 and Figure 3. It can be seen from the table that the three solutions are in reasonable agreement. The expression of pressure rise is computed by employing Mathematica. The graphical results for pressure rise, velocity, temperature, pressure gradient, and stream function are shown in Figures 4 to 18. The graphs of pressure rise Δp against volume flow rate Q for different values of Deborah number Γ and viscosity parameter α are prescribed in Figures 4 and 5. These figures indicate that pressure rise and volume flow rate are inversely proportional to each other. It means that the pressure rise gives larger values for small flow rate and it gives smaller values for large Q. The pressure rise increases with an increase in Γ while it decreases with an increase in α. The peristaltic pumping occurs in the region $-1.5 \leq Q < 0$ for Γ, $-1.5 \leq Q \leq 1.0$ for α, otherwise augmented pumping occurs. The velocity field u for different values of Γ, α, and Q are depicted in Figures 6 to 8. It is noticed that the velocity field increases by increasing Γ and Q. However, near the channel walls, the velocity decreases but in the middle of the channel the velocity increases when α is increased. The temperature field for different values of Ec, Pr, Γ, and α, against space variable y are displayed in Figures 9 to 12. Obviously, by increasing Ec, Pr, Γ, and α, the temperature increases. The variation of pressure gradient are plotted in Figures 13 to 17. These figures show that the pressure gradient is large when $z \in [0, 0.5]$ and $z \in [1, 1.5]$ and small when $z \in [0.51, 0.99]$. Moreover, pressure gradient increases by increasing Γ, α, a, and b and decreases with an increase in ϕ.

The trapping phenomena for different wave shapes such as sinusoidal, triangular, and trapezoidal waves are shown in Figure 18. It is observed that the size of the trapping bolus in the triangular wave is smaller compared to the other waves and also the number of trapping bolus is less in the triangular wave case as compared to the sinusoidal and trapezoidal waves.

5. Conclusion

This study examines the peristaltic flow and heat transfer in a third-order fluid of variable viscosity. Long wavelength assumption is used. The main points of the performed analysis are as follows:

1. The perturbation, homtopy analysis, and numerical solutions are identical up to three digits.

2. The effects of Γ and α on the pressure rise are opposite.

3. The influence of Γ, α, and Q on the velocity is qualitatively similar.

4. Temperature profile increases with an increase in Γ, α, Ec, and Pr.

5. The size of the trapped bolus in the triangular wave is smaller when compared with the trapezoidal and sinusoidal waves.

6. The pressure gradient increases when Γ, α, b, a are increased. It decreases with an increase in ϕ.

Acknowledgement

The authors thank the Higher Education Commission for financial support of this work.

6. Appendix

This section includes the values of L_i $(i = 1-111)$ appearing in (16) and (17).

$$
\begin{aligned}
a_{11} &= -(6h_1^3 + 36Fh_1h_2 + 18h_1^2h_2 - 18h_1h_2^2 - 6h_2^3 \\
&\quad + 6h_1^4\alpha + 24Fh_1^2h_2\alpha + 12h_1^3h_2\alpha + 24Fh_1h_2^2\alpha \\
&\quad - 12h_1h_2^3\alpha - 6h_2^4\alpha + h_1^5\alpha^2 + h_1^4h_2\alpha^2 + h_1^4h_2\alpha^2 \\
&\quad + 12Fh_1^2h_2^2\alpha^2 + 4h_1^3h_2^2\alpha^2 - 4h_1^2h_2^3\alpha^2 - h_1h_2^4\alpha^2 \\
&\quad - h_2^5\alpha^2), \\
a_{12} &= (h_1 - h_2)^3(6 + 6h_1\alpha + 6h_2\alpha + h_1^2\alpha^2 + 4h_1h_2\alpha^2 \\
&\quad + h_2^2\alpha^2), \\
a_{13} &= -(6Fh_1^3 - 18Fh_1^2h_2 - 12h_1^3h_2 - 18Fh_1h_2^2 \\
&\quad + 6Fh_2^3 + 12h_1h_2^3\alpha + 6Fh_1^4\alpha - 12Fh_1^3h_2\alpha \\
&\quad - 12h_1^4h_2\alpha - 24Fh_1^2h_2^2\alpha - 12Fh_1h_2^3\alpha + 6Fh_2^4\alpha \\
&\quad + 12h_2^4h_1\alpha^2 + Fh_1^5\alpha^2 + Fh_1^4h_2\alpha^2 - 2h_1^5h_2\alpha^2 \\
&\quad - 8Fh_1^3h_2^2\alpha^2 - 2h_2^2h_1^4\alpha^2 - 8Fh_1^2h_2^3\alpha^2 + Fh_1h_2^4\alpha^2 \\
&\quad + 2h_1^2h_2^4\alpha^2 + Fh_2^5\alpha^2 + 2h_1h_2^5\alpha^2), \\
a_{14} &= 2(h_1 - h_2)^3(6 + 6h_1\alpha + 6h_2\alpha + h_1^2\alpha^2 \\
&\quad + 4h_1h_2\alpha^2 + h_2^2\alpha^2), \\
L_1 &= \\
&-\frac{36(F + h_1 - h_2)(2 + (h_1 + h_2)\alpha)}{(h_1 - h_2)^3(6 + 6(h_1 + h_2)\alpha + (h_1^2 + 4h_1h_2 + h_2^2)\alpha^2)}, \\
L_2 &= \frac{+\begin{bmatrix} 12(3Fh_1 + 3h_1^2 + 3Fh_2 - 3h_2^2 + 2Fh_1^2\alpha \\ +2h_1^3\alpha + 2Fh_1h_2\alpha + 2Fh_2^2\alpha - 2h_2^3\alpha) \\ (2 + (h_1 + h_2)\alpha) \end{bmatrix}}{\begin{bmatrix} (h_1 - h_2)^3(6 + 6h_1\alpha + 6h_2\alpha + h_1^2\alpha^2 \\ +4h_1h_2\alpha^2 + h_2^2\alpha^2) \end{bmatrix}}, \\
L_3 &= \frac{a_{11}}{a_{12}}, \quad L_4 = \frac{a_{13}}{a_{14}}, \quad L_5 = \alpha^3 L_1^3,
\end{aligned}
$$

$$L_6 = 3L_1^2L_2\alpha^3 + 3\alpha^2L_1^3,$$
$$L_7 = 3L_1L_2^2\alpha^3 + 3\alpha L_1^3 + 9L_1^2L_2\alpha^2,$$
$$L_8 = L_1^3 + L_2^3\alpha^3 + 9L_1^2L_2\alpha + 9L_2^2L_1\alpha^2,$$
$$L_9 = 3L_1^2L_2 + 9\alpha L_1L_2^2 + 3L_2^3\alpha^2,$$
$$L_{10} = 3L_2^2L_1 + 3\alpha L_2^3, \quad L_{11} = L_2^3, \quad L_{12} = -\frac{2\alpha L_5}{72},$$
$$L_{13} = -\frac{L_5}{28} - \frac{\alpha L_6}{28}, \quad L_{14} = -\frac{L_6}{21} - \frac{\alpha L_7}{21},$$
$$L_{15} = -\frac{L_7}{15} - \frac{\alpha L_8}{15}, \quad L_{16} = -\frac{L_8}{10} - \frac{\alpha L_9}{10},$$
$$L_{17} = -\frac{L_9}{6}, \quad L_{18} = \alpha^2L_1^2,$$
$$L_{19} = 2\alpha^2L_1L_2 + 2\alpha L_1^2,$$
$$L_{20} = L_1^2 + \alpha^2L_2^2 + 4\alpha L_1L_2,$$
$$L_{21} = 2L_1L_2 + 2\alpha L_2^2, \quad L_{22} = L_2^2,$$
$$L_{23} = -\alpha E_cP_rL_{18}, \quad L_{24} = E_cP_r(L_{18} - \alpha L_{19}),$$
$$L_{25} = E_cP_r(L_{19} - \alpha L_{20}), \quad L_{26} = E_cP_r(L_{20} - \alpha L_{21}),$$
$$L_{27} = E_cP_r(L_{21} - \alpha L_{22}), \quad L_{28} = -E_cP_rL_{22},$$
$$L_{29} = \frac{L_{23}}{42}, \quad L_{30} = \frac{L_{24}}{30}, \quad L_{31} = \frac{L_{25}}{20},$$
$$L_{32} = \frac{L_{26}}{12}, \quad L_{33} = \frac{L_{27}}{6}, \quad L_{34} = \frac{L_{28}}{2},$$
$$L_{35} = L_{29}h_1^7 + L_{30}h_1^6 + L_{31}h_1^5 + L_{32}h_1^4 + L_{33}h_1^3 + L_{34}h_1^2,$$
$$L_{36} = L_{29}h_2^7 + L_{30}h_2^6 + L_{31}h_2^5 + L_{32}h_2^4 + L_{33}h_2^3 + L_{34}h_2^2,$$
$$L_{37} = \frac{1 - L_{35} + L_{36}}{(h_1 - h_2)}, \quad L_{38} = 1 - L_{35} - L_{37}h_1,$$
$$L_{39} = (L_{18})^2, \quad L_{40} = 2L_{18}L_{19},$$
$$L_{41} = 2L_{18}L_{20} + (L_{19})^2, \quad L_{42} = 2L_{18}L_{21} + 2L_{19}L_{20},$$
$$L_{43} = 2L_{18}L_{22} + 2L_{19}L_{21} + (L_{20})^2,$$
$$L_{44} = 2L_{19}L_{22} + 2L_{20}L_{21},$$
$$L_{45} = 2L_{20}L_{22} + (L_{21})^2, \quad L_{46} = 2L_{21}L_{22},$$
$$L_{47} = (L_{22})^2, \quad L_{48} = -2\alpha L_5,$$
$$L_{49} = -2L_5 - 2\alpha L_6, \quad L_{50} = -2L_6 - 2\alpha L_7,$$
$$L_{51} = -2L_7 - 2\alpha L_8, \quad L_{52} = -2L_8 - 2\alpha L_9,$$
$$L_{53} = -2L_9,$$

$$\begin{aligned} L_{54} = {} & h_1^2h_2^2(6h_1^5L_{12} + 6h_2^5L_{12} + 5h_2^4L_{13} \\ & + 5h_1^4(2h_2L_{12} + L_{13}) + 4h_2^3L_{14} \\ & + 4h_1^3(3h_2^2L_{12} + 2h_2L_{13} + L_{14}) + 3h_2^5L_{15} \\ & + 3h_1^2(4h_2^3L_{12} + 3h_2^2L_{13} + 2h_2L_{14} + L_{15}) \\ & + 2h_2L_{16} + 2h_1(5h_2^4L_{12} + 4h_2^3L_{13} + 3h_2^2L_{14} \\ & + 2h_2L_{15} + L_{16}) + L_{17}), \end{aligned}$$

$$\begin{aligned} L_{55} = {} & -6(7h_1^6L_{12} + 6h_1^5(2h_2L_{12} + L_{13}) \\ & + 5h_1^4(3h_2^2L_{12} + 2h_2L_{13} + L_{14}) \\ & + 4h_1^3(4h_2^3L_{12} + 3h_2^2L_{13} + 2h_2L_{14} + L_{15}) \\ & + 3h_1^2(5h_2^4L_{12} + 4h_2^3L_{13} + 3h_2^2L_{14} \\ & + 2h_2L_{15} + L_{16}) + 2h_1(6h_2^5L_{12} + 5h_2^4L_{13} \\ & + 4h_2^3L_{14} + 3h_2^2L_{15} + 2h_2L_{16} + L_{17}) \\ & + h_2(7h_2^5L_{12} + 6h_2^4L_{13} + 5h_2^3L_{14} + 4h_2^2L_{15} \\ & + 3h_2L_{16} + 2L_{17})), \end{aligned}$$

$$\begin{aligned} L_{56} = {} & 2(6h_1^7L_{12} + h_1^6(24h_2L_{12} + 5L_{13}) \\ & + 4h_1^5(9h_2^2L_{12} + 5h_2L_{13} + L_{14}) \\ & + h_1^4(42h_2^3L_{12} + 29h_2^2L_{13} + 16h_2L_{14} + 3L_{15}) \\ & + 2h_1^3(21h_2^4L_{12} + 16h_2^3L_{13} + 11h_2^2L_{14} \\ & + 6h_2L_{15} + L_{16}) + 4h_2h_1(6h_2^5L_{12} + 5h_2^4L_{13} \\ & + 4h_2^3L_{14} + 3h_2^2L_{15} + 2h_2L_{16} + L_{17}) \\ & + h_2^2(6h_2^5L_{12} + 2h_2^4L_{13} + 5h_2^2L_{13} + 4h_2^3L_{14} \\ & + 3h_2^2L_{15} + 2h_2L_{16} + L_{17}) + h_1^2(36h_2^5L_{12} \\ & + 29h_2^4L_{13} + 22h_2^3L_{14} + 15h_2^2L_{15} + 8h_2L_{16} + L_{17})), \end{aligned}$$

$$\begin{aligned} L_{57} = {} & -h_1h_2(12h_1^6L_{12} + h_1^5(27h_2L_{12} + 10L_{13}) \\ & + h_1^4(36h_2^2L_{12} + 22h_2L_{13} + 8L_{14}) \\ & + h_1^3(39h_2^3L_{12} + 28h_2^2L_{13} + 17h_2L_{14} + 6L_{15}) \\ & + 4h_1^2(9h_2^4L_{12} + 7h_2^3L_{13} + 5h_2^2L_{14} + 3h_2L_{15} + L_{16}) \\ & + 2h_2(6h_2^5L_{12} + 5h_2^4L_{13} + 4h_2^3L_{14} + 3h_2^2L_{15} \\ & + 2h_2L_{16} + L_{17}) + h_1(27h_2^5L_{12} + 22h_2^4L_{13} \\ & + 17h_2^3L_{14} + 12h_2^2L_{15} + 7h_2L_{16} + 2L_{17})), \end{aligned}$$

$$L_{58} = (L_{48})^2, \quad L_{59} = 2L_{48}L_{49},$$
$$L_{60} = 2L_{48}L_{50} + (L_{49})^2, \quad L_{61} = 2L_{48}L_{51} + 2L_{49}L_{50},$$
$$L_{62} = 2L_{48}L_{52} + 2L_{49}L_{51} + (L_{50})^2,$$
$$L_{63} = 2L_{48}L_{53} + 2L_{49}L_{52} + 2L_{50}L_{51},$$
$$L_{64} = 2L_{48}L_{54} + 2L_{50}L_{52} + (L_{51})^2,$$
$$L_{65} = 2L_{49}L_{54} + 2L_{50}L_{53} + 2L_{51}L_{52},$$

$$L_{66} = 2L_{49}L_{55} + 2L_{50}L_{54} + 2L_{51}L_{53} + (L_{52})^2,$$
$$L_{67} = 2L_{51}L_{54} + 2L_{50}L_{55} + 2L_{53}L_{52},$$
$$L_{68} = 2L_{51}L_{55} + 2L_{52}L_{54} + (L_{53})^2,$$
$$L_{69} = 2L_{52}L_{55} + 2L_{54}L_{53}, \quad L_{70} = 2L_{53}L_{55} + (L_{54})^2,$$
$$L_{71} = 2L_{54}L_{55}, \quad L_{72} = (L_{55})^2, \quad L_{73} = E_c P_r \alpha L_{58},$$
$$L_{74} = -E_c P_r (L_{58} - \alpha L_{59}),$$
$$L_{75} = -E_c P_r (L_{59} - \alpha L_{60}),$$
$$L_{76} = -E_c P_r (L_{60} - \alpha L_{61}),$$
$$L_{77} = -E_c P_r (L_{61} - \alpha L_{62}),$$
$$L_{78} = -E_c P_r (L_{62} - \alpha L_{63}),$$
$$L_{79} = -E_c P_r (L_{63} - \alpha L_{64}),$$
$$L_{80} = -E_c P_r (L_{64} - \alpha L_{65} + 2L_{39}),$$
$$L_{81} = -E_c P_r (L_{65} - \alpha L_{66} + 2L_{40}),$$
$$L_{82} = -E_c P_r (L_{66} - \alpha L_{67} + 2L_{41}),$$
$$L_{83} = -E_c P_r (L_{67} - \alpha L_{68} + 2L_{42}),$$
$$L_{84} = -E_c P_r (L_{68} - \alpha L_{69} + 2L_{43}),$$
$$L_{85} = -E_c P_r (L_{69} - \alpha L_{70} + 2L_{44}),$$
$$L_{86} = -E_c P_r (L_{70} - \alpha L_{71} + 2L_{45}),$$
$$L_{87} = -E_c P_r (L_{71} - \alpha L_{72} + 2L_{46}),$$
$$L_{88} = -E_c P_r (L_{72} + 2L_{47}),$$
$$L_{89} = \frac{L_{73}}{272}, \quad L_{90} = \frac{L_{74}}{240}, \quad L_{91} = \frac{L_{75}}{210},$$
$$L_{92} = \frac{L_{76}}{182}, \quad L_{93} = \frac{L_{77}}{156}, \quad L_{94} = \frac{L_{78}}{132},$$
$$L_{95} = \frac{L_{79}}{110}, \quad L_{96} = \frac{L_{80}}{90}, \quad L_{97} = \frac{L_{81}}{72},$$
$$L_{98} = \frac{L_{82}}{56}, \quad L_{99} = \frac{L_{83}}{42}, \quad L_{100} = \frac{L_{84}}{30},$$
$$L_{101} = \frac{L_{85}}{20}, \quad L_{102} = \frac{L_{86}}{12}, \quad L_{103} = \frac{L_{87}}{6},$$
$$L_{104} = \frac{L_{88}}{2},$$
$$\begin{aligned} L_{105} = {} & L_{89}h_1^{17} + L_{90}h_1^{16} + L_{91}h_1^{15} + L_{92}h_1^{14} + L_{93}h_1^{13} \\ & + L_{94}h_1^{12} + L_{95}h_1^{11} + L_{96}h_1^{10} + L_{97}h_1^{9} + L_{98}h_1^{8} \\ & + L_{99}h_1^{7} + L_{100}h_1^{6} + L_{101}h_1^{5} + L_{102}h_1^{4} + L_{103}h_1^{3} \\ & + L_{104}h_1^{2}, \end{aligned}$$
$$\begin{aligned} L_{106} = {} & L_{89}h_2^{17} + L_{90}h_2^{16} + L_{91}h_2^{15} + L_{92}h_2^{14} + L_{93}h_2^{13} \\ & + L_{94}h_2^{12} + L_{95}h_2^{11} + L_{96}h_2^{10} + L_{97}h_2^{9} + L_{98}h_2^{8} \\ & + L_{99}h_2^{7} + L_{100}h_2^{6} + L_{101}h_2^{5} + L_{102}h_2^{4} + L_{103}h_2^{3} \\ & + L_{104}h_2^{2}, \end{aligned}$$
$$L_{107} = \frac{L_{106} - L_{105}}{h_1 - h_2}, \quad L_{108} = -L_{105} - h_1 L_{107},$$
$$L_{109} = \frac{L_1 \alpha}{12}, \quad L_{110} = \frac{L_1}{6} + \frac{L_2 \alpha}{6}, \quad L_{111} = \frac{L_2}{2}.$$

[1] T. W. Latham, Fluid motion in a peristaltic pump, MS. Thesis, Massachusetts Institute of Technology, Cambridge 1966.
[2] E. F. Elshehawey, N. T. Eladabe, E. M. Elghazy, and A. Ebaid, Appl. Math. Comput. **182**, 140 (2006).
[3] T. Hayat, N. Ali, Q. Hussain, and S. Asghar, Phys. Lett. A **372**, 1477 (2008).
[4] A. H. Abd El-Naby and A. E. M. El-Misiery, Appl. Math. Comput. **128**, 19 (2002).
[5] T. Hayat, F. M. Mahomed, and S. Asghar, Nonlinear Dyn. **40**, 375 (2005).
[6] T. Hayat and N. Ali, Appl. Math. Comput. **193**, 535 (2007).
[7] T. Hayat, Y. Wang, A. M. Siddiqui, and K. Hutter, Math. Probl. Eng. **1**, 1 (2003).
[8] T. Hayat and N. Ali, Physica A **371**, 188 (2006).
[9] M. Ealshahed and M. H. Haroun, Math. Probl. Eng. **6**, 663 (2005).
[10] M. H. Haroun, Comput. Mater. Sci. **39**, 324 (2007).
[11] T. Hayat, N. Ali, and Z. Abbas, Phys. Lett. A **370**, 331 (2007).
[12] S. Srinivas and M. Kothandapani, Int. Commun. Heat Mass Tranf. **20**, 514 (2008).
[13] M. Kothandapani and S. Srinivas, Phys. Lett A **372**, 4586 (2008).
[14] S. Nadeem and N. S. Akbar, Commun. Nonlinear Sci. Numer. Simul. **14**, 3844 (2009).
[15] S. Srinivas and M. Kothandapania, Appl. Math. Comp. **213**, 197 (2009).
[16] M. Asif Ikbal, C. Santabrata, and P. K. Mandal, Appl. Math. Comp. **201**, 16 (2008).